

# Magnetism and band structure of the semimagnetic semiconductor Pb-Sn-Mn-Te

T. Story, G. Karczewski, L. Świerkowski, and R. R. Gałazka

*Institute of Physics, Polish Academy of Sciences, aleja Lotników 32/46, PL-02-668 Warsaw, Poland*

(Received 21 May 1990)

Measurements of magnetization, magnetic susceptibility, specific heat, and Hall effect of the  $\text{Pb}_{1-x-y}\text{Sn}_x\text{Mn}_y\text{Te}$  semimagnetic semiconductor ( $x=0.72$ ,  $y=0.03$  and  $x=0.64$ ,  $y=0.03$ ) were performed in samples with different concentration of carriers ( $p=8\times 10^{19}$  to  $1.4\times 10^{21}\text{ cm}^{-3}$ ). A low-temperature ferromagnetic phase was established in the samples with carrier concentration larger than a threshold value  $p_t=3\times 10^{20}\text{ cm}^{-3}$ . Samples with lower carrier concentrations are paramagnetic in the whole temperature range studied ( $T=1.5\text{--}300\text{ K}$ ). The carrier-concentration dependence of the Curie temperature has an unusual thresholdlike character. The explanation of this effect is based on the Ruderman-Kittel-Kasuya-Yosida (RKKY) indirect exchange interaction between Mn spins and a two-valence-band model of the band structure of  $\text{Pb}_{1-x-y}\text{Sn}_x\text{Mn}_y\text{Te}$ . Theoretical calculations based on the experimentally determined parameters of the band structure are presented. The results show that the most important role in the RKKY interaction is played by heavy holes from the  $\Sigma$  band located 185 meV below the top of the  $L$  band of light holes.

## I. INTRODUCTION

In this paper we present results of experimental and theoretical studies of magnetic and electron properties of the  $\text{Pb}_{1-x-y}\text{Sn}_x\text{Mn}_y\text{Te}$  semimagnetic alloy. This material is a substitutional solid solution in which paramagnetic  $\text{Mn}^{2+}$  ions are randomly distributed in a metal fcc sublattice of the rock-salt crystal lattice of Pb-Sn-Mn-Te. The host material is a well-known semiconducting alloy  $\text{Pb}_{1-x}\text{Sn}_x\text{Te}$  which can be grown with arbitrary composition. The solubility of manganese in the matrix of Pb-Sn-Te is rather high and homogeneous samples with manganese content about 20 at. % can be grown using the Bridgman method.

Our investigations were carried out on the samples with a large tin telluride content ( $x>0.5$ ) and a small concentration of manganese ions ( $y=0.03$ ). The main constituent of the alloy, i.e., SnTe, practically determines the electron properties of the material. The typical carrier concentration is very high ( $p=10^{20}\text{--}10^{21}\text{ cm}^{-3}$ ). Carriers are generated by metal vacancies and their number is temperature independent. Only  $p$ -type conductivity is observed. There is the possibility to control the number of carriers by annealing. The band structure of Pb-Sn-Mn-Te is analogous to the band structure of the host material Pb-Sn-Te. The energy gap is narrow and, consequently, the energy dispersion relations of carriers in the conduction and valence bands are nonparabolic. Approximately 185 meV below the top of the main valence band there is a band of heavy holes at the  $\Sigma$  point of the Brillouin zone.<sup>1</sup>

Pb-Sn-Mn-Te belongs to the family of Mn-based IV-VI semimagnetic compound semiconductors (SMSC) which consists of the following mixed crystals: Pb-Mn-Te, Pb-Mn-Se, Pb-Mn-S, Sn-Mn-Te, Ge-Mn-Te, Pb-Sn-Mn-Se, and Pb-Ge-Mn-Te.<sup>2-4</sup> In all these alloys,  $\text{Mn}^{2+}$  ions conserve their localized spin magnetic moments ( $S=\frac{5}{2}$ ) after the incorporation into the IV-VI matrix. The host

materials are weak diamagnets with a typical magnetic susceptibility about  $\chi=-3\times 10^{-7}\text{ emu/g}$ . The magnetic properties of Pb-Sn-Mn-Te are determined by  $\text{Mn}^{2+}$  ions.

From the point of view of magnetic properties IV-VI SMSC divide into two groups of materials. The first group (Pb-Mn-Te, Pb-Mn-Se, Pb-Mn-S, and Pb-Sn-Mn-Se) is characterized by relatively low concentration of carriers ( $10^{17}\text{--}10^{19}\text{ cm}^{-3}$ ). These materials are paramagnetic in the temperature range  $T=1\text{--}300\text{ K}$ . The existence of a weak antiferromagnetic interaction is experimentally observed in the temperature dependence of the magnetic susceptibility and temperature and magnetic field dependence of the magnetization.<sup>5,6</sup> A superexchange interaction via anions is responsible for this antiferromagnetic interaction between manganese ions. It is believed that conducting carriers play no important role in the interpretations of the magnetic properties of these materials. At very low temperatures ( $T<1\text{ K}$ ), the existence of a spin-glass phase was reported for Pb-Mn-Te.<sup>7</sup>

The second group of IV-VI SMSC (Sn-Mn-Te, Ge-Mn-Te, and Pb-Ge-Mn-Te with a large content of Ge) has completely different low-temperature magnetic properties. A ferromagnetic ordering is observed in magnetic and specific-heat measurements.<sup>8-13</sup> The indirect exchange interaction via free carriers [Ruderman-Kittel-Kasuya-Yosida (RKKY) interaction] is responsible for the formation of the ferromagnetic phase. This dramatic differences between the low-temperature magnetic properties of these two groups of SMSC is due to the significant difference in the carrier concentration.

The purpose of our paper is to study the influence of the carrier concentration on the magnetic properties of SMSC in the material in which we can control the number of carriers in the range characteristic for both above-mentioned groups of IV-VI (SMSC). We expect that, in this way, we can also experimentally study the influence of electron parameters of SMSC on their magnetic properties.

The important point of our investigations is the choice of a model material for the studies. We have chosen the quaternary mixed crystal  $\text{Pb}_{1-x-y}\text{Sn}_x\text{Mn}_y\text{Te}$  with a large content of tin and a small concentration of manganese. Based on the results of the experimental investigations of Sn-Mn-Te, we expect that the number of carriers in our material will be large enough to make the RKKY mechanism responsible for the magnetic properties of high-carrier-concentration samples of Pb-Sn-Mn-Te. On the other hand, the use of the mixed crystal of  $\text{Pb}_{1-x}\text{Sn}_x\text{Te}$  as a host material should allow us to obtain (by annealing) samples with a relatively low concentration of carriers. In such a system we can observe how, with decreasing carrier concentration, the ferromagnetic RKKY interaction switches off and the system becomes dominated by the antiferromagnetic interactions. This paper is a continuation of our two previous short works.<sup>14,15</sup>

## II. CHARACTERIZATION OF SAMPLES

We investigated  $\text{Pb}_{1-x-y}\text{Sn}_x\text{Mn}_y\text{Te}$  samples with the following chemical compositions:  $x=0.72$ ,  $y=0.03$  and  $x=0.64$ ,  $y=0.03$ . The crystals were grown by a vertical Bridgman method. The chemical composition of our samples was checked by an electron microprobe which revealed good chemical homogeneity of the material. The concentration of  $\text{Mn}^{2+}$  ions is practically constant along an ingot. The composition of tin changes standardly according to the thermodynamic phase diagram. The x-ray measurements showed that Pb-Sn-Mn-Te crystallizes in the rock-salt crystal lattice. The lattice constant at room temperature is equal to  $a_0=6.331$  Å (as-grown samples with  $x=0.72$ , hole concentration  $p=7 \times 10^{20} \text{ cm}^{-3}$ ). No second-phase inclusions were observed. Our samples usually consist of a few small disoriented monocrystalline grains. We have not obtained any experimental evidence for the low-temperature structural phase transition from the rock-salt to rhombohedral phases usually observed in the host material Pb-Sn-Te.

dc transport measurements performed on the samples of Pb-Sn-Mn-Te revealed their good electrical homogeneity. As-grown samples have the concentrations of holes  $p=7 \times 10^{20} \text{ cm}^{-3}$  (crystal with  $x=0.72$ ) and  $p=3 \times 10^{20} \text{ cm}^{-3}$  (crystal with  $x=0.64$ ). All studied samples were  $p$  type. Using the method of isothermal annealing, we could control the number of holes in the range  $p=8 \times 10^{19}$  to  $1.4 \times 10^{21} \text{ cm}^{-3}$ .<sup>16</sup> In this paper all samples of Pb-Sn-Mn-Te are characterized by the low-temperature Hall concentrations  $p=1/eR_H$ , where  $R_H$  is the low-field Hall constant. The relation between the Hall concentration and the real concentration of holes ( $p_0$ ) is discussed in Sec. V of this work.

## III. MAGNETIC PROPERTIES

To experimentally study the magnetic properties of Pb-Sn-Mn-Te we performed measurements of magnetization, magnetic susceptibility, specific heat, and the Hall effect in the samples of  $\text{Pb}_{0.25}\text{Sn}_{0.72}\text{Mn}_{0.03}\text{Te}$  and

$\text{Pb}_{0.33}\text{Sn}_{0.64}\text{Mn}_{0.03}\text{Te}$  with different concentrations of carriers. Magnetization and magnetic susceptibilities were studied by several experimental techniques. High-temperature and high-magnetic-field measurements (temperature range  $T=2-300$  K, magnetic field range  $B \leq 5$  T) were done using a SQUID magnetometer of Francis Bitter National Magnet Laboratory. Low-temperature and low-dc magnetic field data (temperature range  $T=1.5-4.2$  K, magnetic field  $B \leq 0.15$  T) were obtained by means of a simple homemade flux-metric magnetometer. Specific-heat measurements were done in the temperature range  $T=1.5-60$  K by standard heat-pulse technique. The results of these measurements will be presented below, first for samples of Pb-Sn-Mn-Te with a relatively low concentration of carriers  $p < 3 \times 10^{20} \text{ cm}^{-3}$  and then for high carrier-concentration samples ( $p \geq 3 \times 10^{20} \text{ cm}^{-3}$ ).

### A. Magnetic properties of low-carrier-concentration samples

The magnetic susceptibility of several samples of Pb-Sn-Mn-Te with a carrier concentration in the range  $p=8 \times 10^{19}$  to  $3 \times 10^{20} \text{ cm}^{-3}$  were studied. A typical result of the temperature dependence of the inverse magnetic susceptibility of Pb-Sn-Mn-Te with a low carrier concentration is presented in Fig. 1(a). One can see that, according to the Curie-Weiss law, the plot of  $\chi^{-1}(T)$  follows the straight line in a wide temperature range with the paramagnetic Curie temperature  $\theta=0 \pm 0.2$  K. In the region of high temperatures, the experimental points bend up from the straight line. This effect is due to the

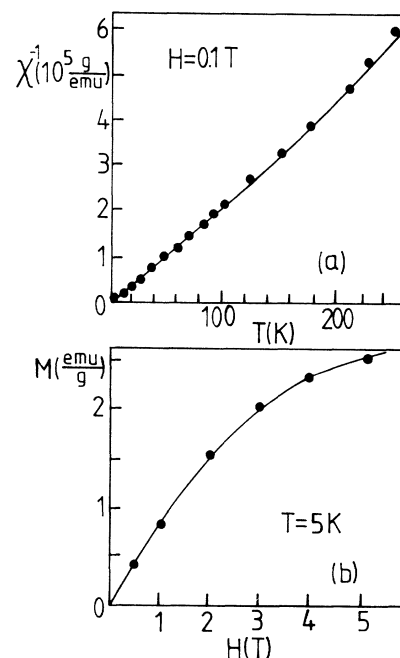


FIG. 1. The temperature dependence of the inverse magnetic susceptibility of the sample of  $\text{Pb}_{0.25}\text{Sn}_{0.72}\text{Mn}_{0.03}\text{Te}$  with a carrier concentration  $p=1.4 \times 10^{20} \text{ cm}^{-3}$  (a). (b) presents the magnetic-field dependence of the magnetization of the same sample. The solid lines are theoretical descriptions based on the Curie law and Brillouin function, respectively.

temperature-independent diamagnetic contribution of the host material Pb-Sn-Te. The best-fitted value of this concentration is equal to  $\chi_d = -2.3 \times 10^{-7}$  emu/g. The solid line presented in Fig. 1(a) is a theoretical description of the experimental data based on the simple equation

$$\chi(T) = \chi_d + C / (T - \theta),$$

where

$$C = N_{\text{Mn}} S(S+1) g_{\text{Mn}}^2 \mu_B^2$$

is the Curie constant and  $\theta$  is the paramagnetic Curie temperature. The number of manganese ions which can be derived from the value of the Curie constant (assuming  $S = \frac{5}{2}$  and  $g_{\text{Mn}} = 2$ ) is equivalent to the composition  $3 \pm 0.2$  at.% and agrees very well with the technological composition. The results of measurements of other samples of Pb-Sn-Mn-Te with a low concentration of holes showed that, in this range of carrier concentrations, the paramagnetic Curie temperature seems to be weakly carrier-concentration dependent. In Fig. 1(b) the magnetic-field dependence of magnetization at temperature  $T = 5$  K is presented for the same sample. One can see that the experimental points are described by the Brillouin function ( $S = \frac{5}{2}$ ) with the magnetic saturation moment  $M_s = 2.86$  emu/g. The value expected from the technological data is equal to  $M_s = 3.0$  emu/g.

Concluding the experimental data for Pb-Sn-Mn-Te samples with a carrier concentration  $p < 3 \times 10^{20} \text{ cm}^{-3}$ , one can say that a good theoretical description of the magnetic properties of these samples may be obtained based on the standard formulas for the system of very weakly coupled magnetic moments. In the temperature range studied ( $T = 1.5 - 300$  K), low-carrier-concentration samples of Pb-Sn-Mn-Te are paramagnetic.

### B. Magnetic properties of high-carrier-concentration samples

Low-temperature magnetic properties of the samples of Pb-Sn-Mn-Te with a carrier concentration  $p \geq 3 \times 10^{20} \text{ cm}^{-3}$  are qualitatively different than those presented above. A typical plot of the temperature dependence of the inverse magnetic susceptibility is presented in Fig. 2.

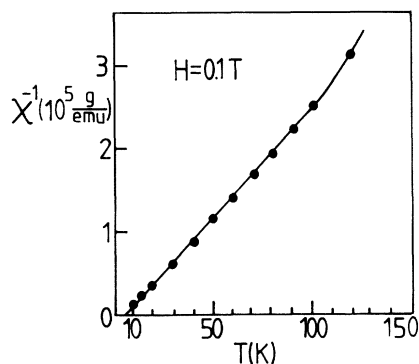


FIG. 2. The plot of the inverse magnetic susceptibility of the sample of  $\text{Pb}_{0.25}\text{Sn}_{0.72}\text{Mn}_{0.03}\text{Te}$  ( $p = 7 \times 10^{20} \text{ cm}^{-3}$ ) as a function of temperature. The solid line follows the Curie-Weiss law.

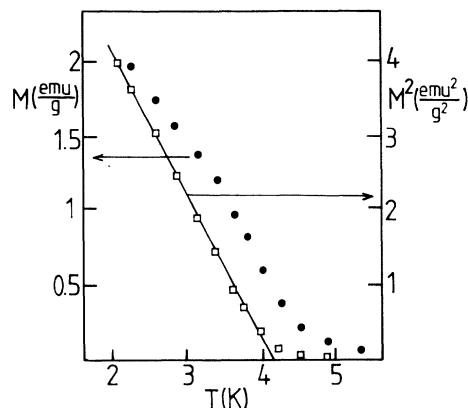


FIG. 3. The temperature dependence of the low-field magnetization of the sample of  $\text{Pb}_{0.25}\text{Sn}_{0.72}\text{Mn}_{0.03}\text{Te}$  ( $p = 7 \times 10^{20} \text{ cm}^{-3}$ ,  $T_c = 4.1$  K) in the critical-temperature region. The  $M(T) \sim (T_c - T)^{1/2}$  law is obeyed below the Curie point and results in the straight-line dependence of the square of the magnetization on the temperature.

One can see that, in the region of high temperatures, the experimental data follow the Curie-Weiss law. However, in contrast to the low-carrier-concentration samples, the paramagnetic Curie temperature is not equal to zero and has a positive value of about  $\theta \approx 4$  K. This result shows that there is a ferromagnetic interaction between Mn spins in Pb-Sn-Mn-Te and this material could no longer be treated as a system of noninteracting magnetic moments. Similar to the paramagnetic samples, the concentration of manganese spins determined based on the value of Curie constant agrees well with technological data.

Figure 3 presents the temperature dependence of the low-magnetic-field magnetization of the sample of  $\text{Pb}_{0.25}\text{Sn}_{0.72}\text{Mn}_{0.03}\text{Te}$  with a carrier concentration  $p = 7 \times 10^{20} \text{ cm}^{-3}$ . One can see that, below a certain critical temperature, magnetization starts to increase very rapidly with decreasing temperature. In the temperature interval of a few tenths of a degree of K, the magnetic moment increases about 1 order of magnitude. The amplitude of this effect increases with lowering the magnetic field used in the process of measurement. Below the critical temperature ( $T \leq T_c$ ), the temperature dependence of magnetization follows the law  $M(T) \sim (T_c - T)^{1/2}$  (see the straight line in Fig. 3). We applied this formula to the phenomenological determination of the ferromagnetic Curie temperature ( $T_c$ ) based on the extrapolation of the low-field  $M^2(T)$  plot to zero values of magnetization. The temperature and magnetic-field dependence of the magnetization of Pb-Sn-Mn-Te below and above the Curie point are presented in Fig. 4. One can see that, at temperatures well below the Curie point, the effect of a quick saturation of the magnetization is observed. The magnetic field of  $B = 0.02$  T is practically enough to saturate the magnetic moment of the sample. A narrow hysteresis loop is observed at temperatures well below the Curie point [see Fig. 4(b)]. All the experimental findings described above are clear evidence for the existence of the low-temperature ferromagnetic phase in the samples of Pb-Sn-Mn-Te with a high concentration of carriers.

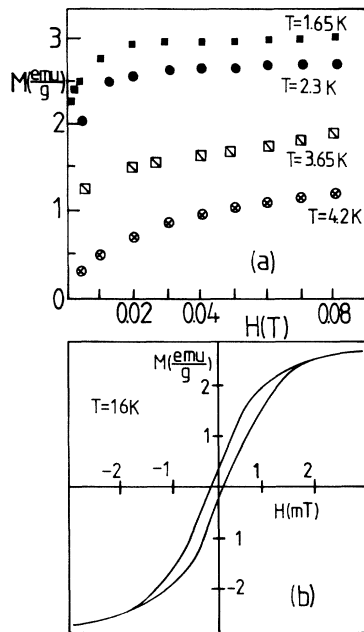


FIG. 4. The magnetic-field dependence of the magnetization of Pb-Sn-Mn-Te ( $T_c = 4.1$  K) at temperatures above and below the Curie point. (b) presents the hysteresis loop observed in this material at low temperatures.

### C. Specific heat

To study the nature of the magnetic phase transition observed at helium temperatures in Pb-Sn-Mn-Te samples with high carrier concentrations, we performed measurements of the specific heat of this material. The temperature dependence of the magnetic contribution to the total specific heat of  $\text{Pb}_{0.25}\text{Sn}_{0.72}\text{Mn}_{0.03}\text{Te}$  with a carrier concentration  $p = 7 \times 10^{20} \text{ cm}^{-3}$  is presented in Fig. 5. This contribution was determined as the difference between the experimentally measured total specific heat and lattice contribution. The latter is determined based on the high-temperature experimental data. A pronounced peak in the temperature dependence of the magnetic

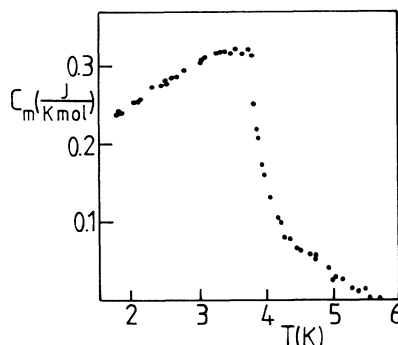


FIG. 5. The magnetic contribution to the total specific heat of the ferromagnetic sample of  $\text{Pb}_{0.25}\text{Sn}_{0.72}\text{Mn}_{0.03}\text{Te}$  ( $p = 7 \times 10^{20} \text{ cm}^{-3}$ ,  $T_c = 4.1$  K).

specific heat is observed at temperature  $T = 3.8$  K which correlates well with the magnetic data ( $T_c = 4.1$  K). This result confirms what we have to do with the second-order magnetic phase transition from a paramagnetic to ferromagnetic state.

We also studied the specific heat of two samples of Pb-Sn-Mn-Te with a low carrier concentration  $p = 1.1 \times 10^{20} \text{ cm}^{-3}$  and  $p = 2.8 \times 10^{20} \text{ cm}^{-3}$ . Paramagnetic Curie temperatures of these samples are equal to  $\theta = 0$  and  $1$  K, respectively.<sup>17</sup> In agreement with the magnetic data, there is no peak on the temperature characteristics of the magnetic contribution to the specific heat of these paramagnetic samples. However, at temperatures below  $T \approx 3$  K, we clearly observed a significant magnetic contribution to the total specific heat of these samples (see Fig. 6). Despite the difference in the carrier concentration and paramagnetic Curie temperature, the temperature dependence of the magnetic specific heat of both of these samples is similar. This result suggests that the observed magnetic contribution is not a high temperature tail of the magnetic phase transition which takes place well below  $T = 1$  K. In our opinion, the magnitude of this effect is too large and the increase of the magnetic specific heat with decreasing temperature too fast to be attributed to any kind of clusters discussed in SMSC.<sup>18</sup> Rather, one could attribute this effect to the system of single  $\text{Mn}^{2+}$  ions, degeneracy of the ground state of which is lifted due to, e.g., the effect of crystal field, or the influence of the magnetic field of a cloud of spin-polarized free carriers surrounding each magnetic ion. Such a system is the source of a Schottky-type anomaly in the specific heat and can correctly describe both the magnitude and the temperature dependence of the observed effect. Numerical estimations show that the splitting of the ground state of  $\text{Mn}^{2+}$  ions should be equal  $\Delta \approx 0.3$  K. There is no final interpretation of this effect as yet.

### D. Carrier-concentration dependence of the Curie temperature

We studied the magnetic properties of the samples of Pb-Sn-Mn-Te with different concentrations of holes. The strong effect of the carrier-concentration dependence of

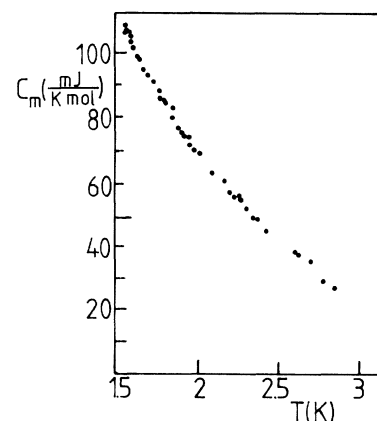


FIG. 6. The temperature dependence of the magnetic contribution to the total specific heat of the paramagnetic sample of Pb-Sn-Mn-Te ( $p = 1.4 \times 10^{20} \text{ cm}^{-3}$ ,  $T_c \approx 0$  K).

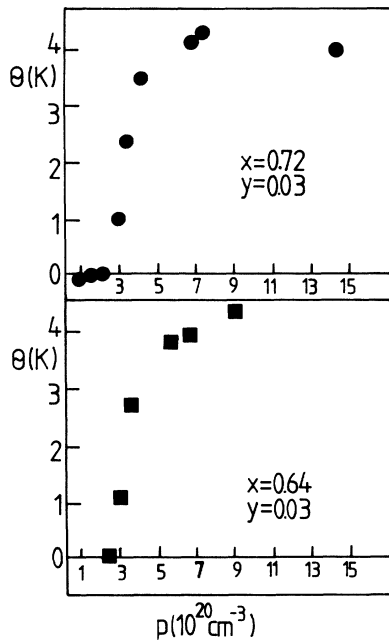


FIG. 7. The carrier-concentration dependence of the paramagnetic Curie temperature of the  $\text{Pb}_{0.25}\text{Sn}_{0.72}\text{Mn}_{0.03}\text{Te}$  and  $\text{Pb}_{0.33}\text{Sn}_{0.64}\text{Mn}_{0.03}\text{Te}$  alloys.

the paramagnetic Curie temperature was established. As one can see in Fig. 7, the thresholdlike hole concentration dependence of the paramagnetic Curie constant is observed in both  $\text{Pb}_{0.25}\text{Sn}_{0.72}\text{Mn}_{0.03}\text{Te}$  and  $\text{Pb}_{0.33}\text{Sn}_{0.64}\text{Mn}_{0.03}\text{Te}$  alloys. The threshold carrier concentration  $p_t = 3 \times 10^{20} \text{ cm}^{-3}$  is practically the same for both alloys. Samples with carrier concentrations lower than this threshold value are paramagnets. Samples of Pb-Sn-Mn-Te with carrier concentrations higher than this value become ferromagnetic at low temperatures. The Curie point of this phase transition depends on the concentration of holes in the way presented in Fig. 7. The measurements performed on samples with the highest obtained concentrations of holes show that, in this range of carrier concentrations, the Curie temperature decreases slightly with an increasing carrier concentration. It is possible to change the low-temperature magnetic properties of each sample of Pb-Sn-Mn-Te controlling its carrier concentration by annealing. A sample which initially (as-grown) was ferromagnetic at helium temperatures can be paramagnetic after the annealing. This process is reversible.

The strong carrier-concentration dependence of the magnetic properties of Pb-Sn-Mn-Te and low concentrations of magnetic ions (i.e., large mean distance between  $\text{Mn}^{2+}$  ions) clearly suggest that the physical mechanism responsible for the formation of the ferromagnetic phase in Pb-Sn-Mn-Te is the indirect exchange interaction via free carriers (RKKY). This mechanism is sufficiently long range and strong enough in high-carrier-concentration samples. However, the theoretical analysis of this idea shows that there are serious qualitative

discrepancies between results of simple RKKY interaction-based calculations and experimental data. In Fig. 8 we present results of the theoretical calculations of the paramagnetic Curie temperature of the Pb-Sn-Mn-Te alloys assuming that the role of carriers effective in the process of RKKY interactions plays light holes from the  $L_6^-$  valence band (i.e., carriers usually responsible for the electron properties of SnTe-based Pb-Sn-Te alloys). The details of these calculations will be presented in the next section. The important result is that there is no possibility to explain the thresholdlike  $T_c(p)$  dependence. In samples with the lowest studied concentration of holes ( $p = 8 \times 10^{19} \text{ cm}^{-3}$ ), the RKKY mechanism predicts the Curie point about 60% of its maximum value (i.e., we should observe  $\theta \approx 3 \text{ K}$  in our samples.) Experimentally we do not see any ferromagnetic phase down to  $T = 1.5 \text{ K}$  and the paramagnetic Curie temperature of these samples is practically zero. The important impulse to the qualitative solution of this problem provided the studies of the influence of hydrostatic pressure on the magnetic properties of Pb-Sn-Mn-Te.<sup>19</sup> It was demonstrated that the application of a relatively low hydrostatic pressure of 10 kbar can even double the value of the Curie temperature of the samples of Pb-Sn-Mn-Te with  $p = p_t$ , whereas, at the same time, no effect or even the effect of an opposite sign was observed in high-carrier-concentration samples. The conclusion of this work was that the important role in the interpretation of the magnetic properties of Pb-Sn-Mn-Te plays two kinds of carriers: light holes from the  $L_6^-$  band and heavy holes from the  $\Sigma$  band. The first correct interpretation of the thresholdlike dependence of the Curie temperature was presented in Ref. 20. The main idea of this work is that, due to the large effective mass of heavy holes, the RKKY interaction is mostly mediated via carriers populating the  $\Sigma$  band. The contribution of the light holes is negligible due to the low effective mass of these carriers. Within the framework of this model, the thresholdlike character of the  $T_c(p)$  dependence has a simple physical interpretation. The threshold hole concentration equals to the concentration of carriers at which the Fermi level enters into the band

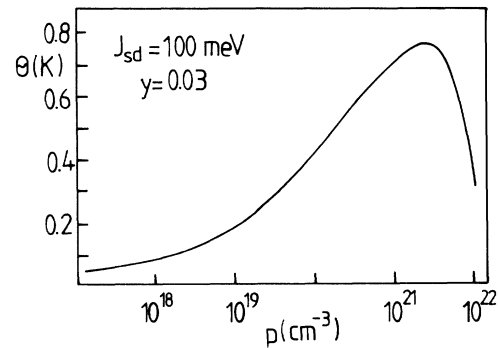


FIG. 8. The carrier-concentration dependence of the paramagnetic Curie temperature of the IV-VI semimagnetic alloy in which the exchange integral is determined by the RKKY interaction via light holes. Calculations were done for band parameters characteristics of the  $\text{Pb}_{0.25}\text{Sn}_{0.72}\text{Mn}_{0.03}\text{Te}$  alloy:  $E_g = 275 \text{ meV}$ ,  $a_0 = 6.331 \text{ \AA}$ , and  $J_{sd} = 100 \text{ meV}$ .

of heavy holes. Due to the presence of these carriers, the strength of the RKKY interaction strongly increases.

Model calculations presented in Ref. 20 are based on rather arbitrary chosen parameters of the band structure of Pb-Sn-Mn-Te. In the next two sections of our paper we will present the experimental arguments for the existence of the band of heavy holes in Pb-Sn-Mn-Te and the results of quantitative analysis of the RKKY interaction based on the experimentally determined band parameters.

#### IV. BAND STRUCTURE OF Pb-Sn-Mn-Te

The existence of heavy carriers, which, according to Ref. 20, are responsible for magnetic properties of Pb-Sn-Mn-Te, were recently confirmed experimentally in transport and optical measurements.<sup>15,21</sup> The temperature and hydrostatic pressure dependence of the Hall constant exhibit characteristic behaviors standardly observed in the case of the two-carrier transport in IV-VI semiconductors. The Hall constant does not depend on temperature in the temperature range  $T = 4.2 \times 100$  K. At higher temperatures, a monotonic increase of the Hall constant is observed. The magnitude of this effect is carrier-concentration dependent. The strongest increase of the Hall constant (about 75%) is observed for a sample with a carrier concentration  $p = 3 \times 10^{20} \text{ cm}^{-3}$  [see Fig. 9(a)]. The behavior of the Hall constant presented above is usually interpreted in IV-VI semiconductors as the result of a two-carrier transport mechanism and a temperature-induced redistribution of carriers between

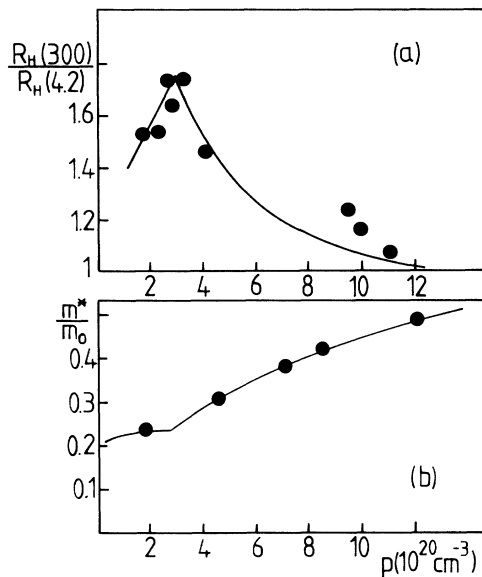


FIG. 9. The carrier-concentration dependence of the ratio of the high- to low-temperature Hall constant (a) and the effective mass of holes (b) in  $\text{Pb}_{0.25}\text{Sn}_{0.72}\text{Mn}_{0.03}\text{Te}$ . The characteristic carrier concentration observed on both plots is equal to the threshold concentration of carriers observed in the magnetic properties of these materials. The experimentally measured effective mass of holes ( $m^*$ ) is a reduced effective mass defined in the case of a two-carrier transport as  $p/m^* = p_L/m_L + p_S/m_S$ , where  $m_L$  and  $m_S$  are the effective masses of the conductivity of light and heavy holes, respectively.

the two valence bands. At a concentration of carriers at which the maximum is observed, the Fermi level enters into the band of heavy holes and these carriers start to participate in the processes of charge transport. It is important that the characteristic concentration of holes observed in the magnetic properties ( $p_i$ ) is equal to the concentration of holes at which the maximum influence of temperature on the Hall constant is observed. In Fig. 9(b) the carrier-concentration dependence of the effective mass of carriers, as obtained from plasma reflectivity measurements,<sup>21</sup> is presented. One can see that, based on the concept of two-carrier transport, it is possible to obtain a good theoretical description of the experimental curve. In the case of both transport and optical data, the characteristic concentration of holes observed in electron properties agrees very well with the threshold concentration of carriers observed in magnetic measurements. This result strongly supports the idea of the two-carrier RKKY interaction as a physical origin of the magnetic properties of Pb-Sn-Mn-Te.

Based on the experimental findings presented above and taking into account the low concentration of manganese ions in our samples, we expect that the model of the band structure of Pb-Sn-Mn-Te similar to the model of the band structure of the nonmagnetic host should provide a good base for a theoretical description of both transport, optical, and magnetic experimental data. This model is presented in Fig. 10. The band of light holes ( $L_6^-$ ) and the band of electrons ( $L_6^+$ ) are located at the  $L$  point of the Brillouin zone and are separated by a relatively narrow direct energy gap. There are four other far bands located at the same point of the Brillouin zone. There are four equivalent energetical valleys of these bands. Approximately 185 meV below the top of the

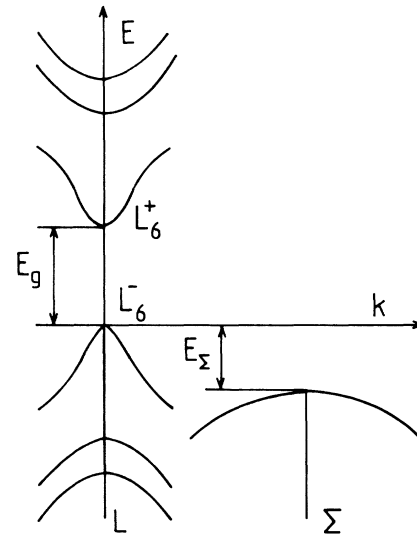


FIG. 10. A model of the band structure of Pb-Sn-Mn-Te. The set of the 2+4 bands at the  $L$  point of the Brillouin zone is described by the Dimmock model. The band of heavy holes is parabolic and isotropic. For  $\text{Pb}_{0.25}\text{Sn}_{0.72}\text{Mn}_{0.03}\text{Te}$ , the values of the band parameters obtained by us are  $E_g = 285$  meV,  $E_S = 185$  meV.

main ( $L_6^-$ ) valence band there is a band of heavy holes ( $\Sigma$ ). This band is located at the  $\Sigma$  point of the Brillouin zone and has 12 equivalent valleys. The parameters of the model as the energy gap ( $E_g$ ), energy separation between the valence bands ( $E_\Sigma$ ), and the effective mass of heavy holes ( $m_\Sigma$ ) generally depend on the concentration of manganese and should be experimentally determined. In our calculations we assume that the main effect of manganese on the band of light holes is due to the change of the energy gap. We also assume that the incorporation of 3 at.% of Mn does not influence the matrix elements of momentum. The anisotropy of the  $L_6^-$  band of light holes was assumed to be the same as in the case of non-magnetic host  $\text{Pb}_{0.28}\text{Sn}_{0.72}\text{Te}$ .

The parameters of the model  $E_g$ ,  $E_\Sigma$ , and the effective mass of heavy holes  $m_\Sigma$  were determined experimentally and are equal:  $E_g = 285 \pm 25$  meV,  $E_\Sigma = 185 \pm 25$  meV and  $m_\Sigma = 1.7 \pm 0.3 m_0$ .<sup>15,21</sup> The energy gap was determined based on the results of measurements of the effective mass of light holes. In narrow-gap semiconductors with a non-parabolic energy dispersion relation, these parameters are related through the matrix element of momentum. However, due to the fact that, experimentally, we obtain the value of the effective mass of conductivity at the Fermi level and to determine the energy gap we need the value of the effective mass at the edge of the band, the calculations are not straightforward and the parameter is determined with low accuracy. The details of calculations and discussion of the problem of the experimental determination of the band parameters of Pb-Sn-Mn-Te are presented in Ref. 22. The position of the band of heavy holes in the band structure of Pb-Sn-Mn-Te was determined based on the results of transport and optical data. The energy  $E_\Sigma$  is equal to the Fermi energy in the samples of Pb-Sn-Mn-Te with a threshold carrier concentration  $p_t = 3 \times 10^{20} \text{ cm}^{-3}$ . The value of the Fermi energy as a function of carrier concentration can be calculated based on the energy dispersion model we describe below. The effective mass of heavy holes was determined in a one-parameter fitting procedure in the theoretical description of the experimentally determined effective mass of carriers. This parameter determines the rate with which the plasma frequency of Pb-Sn-Mn-Te increases with increasing carrier concentration.<sup>22</sup>

The theoretical description of the set of 2 + 4 bands at the  $L$  point of the Brillouin zone is based on the well-known Dimmock model. This model takes into account nonparabolicity and anisotropy of the conduction and valence bands and the influence of far bands on the effective masses of carriers. We use the set of parameters of the Dimmock model providing the best description of the electron properties in the whole range of compositions of  $\text{Pb}_{1-x}\text{Sn}_x\text{Te}$  alloy:<sup>23</sup>

$$\begin{aligned} \frac{P_t^2}{2m_0} &= 5.6 \text{ eV}, & \frac{P_l^2}{2m_0} &= 0.52 \text{ eV}, \\ \frac{m_0}{m_t^-} &= 9.6, & \frac{m_0}{m_l^-} &= 1.2, \\ \frac{m_0}{m_t^+} &= 7.5, & \frac{m_0}{m_l^+} &= 0.7. \end{aligned} \quad (1)$$

Here  $P_{t,l}$  is a transverse and longitudinal matrix element of momentum,  $m_{t,l}^\pm$  are the parameters describing the far band's contribution to the effective mass of holes (+) and electrons (-). The model also includes the band gap  $E_g$  as a parameter which depends on the chemical composition of the alloy.

In the case of the Pb-Sn-Mn-Te alloy, the Dimmock model predicts the following energy dispersion relation for holes in the  $L_6^-$  band:

$$\frac{E}{E_g} = -\frac{1}{2} - \alpha \kappa^2 + [(\beta^2 \kappa^2 - \frac{1}{2})^2 + \kappa^2]^{1/2}, \quad (2)$$

where  $\alpha$  and  $\beta$  are the numerical parameters directly related to the parameters of the Dimmock model and  $\kappa$  is the reduced wave vector.<sup>22</sup> The zero of the energy is at the top of the valence band. This form of the energy dispersion relation is a simplified version of a general solution of the Dimmock model valid in the case when the following conditions are satisfied:

$$\frac{P_t^2}{P_l^2} = \frac{m_t^+}{m_l^+} = \frac{m_t^-}{m_l^-}. \quad (3)$$

These conditions are reasonably well satisfied in the Pb-Sn-Te alloys [see the numerical values of parameters in Eq. (1)]. Physically they mean that the anisotropy of the band of light holes  $L_6^-$  is the same as the anisotropy of the far-band contributions to the effective mass of holes in this band. In our opinion, this approximation does not influence the results of the calculations at the precision level we are dealing with comparing theoretical calculations with experimental data. The same relation transforms the Dimmock's dispersion relation to the form dependent only on the modulus of the reduced wave vector. This allows us to perform calculations in an analytical way. The dispersion relation (2) transforms itself into the well-known Kane dispersion relation for IV-VI alloys in the special case when  $\alpha = \beta = 0$ .

Due to the large direct energy gap at the  $\Sigma$  point of the Brillouin zone of the Pb-Sn-Te alloys, the energy dispersion relation of heavy holes is parabolic. In our calculations we also assume that this is an isotropic band.

Based on the energy dispersion relation (2), we calculated the carrier-concentration dependence of the Fermi level and distribution of holes between two valence bands. The results of these calculations are presented in Fig. 11. One can notice that, due to high density of states connected with the band of heavy holes, the Fermi level is practically constant for samples with a concentration of holes higher than  $p_t = 3 \times 10^{20} \text{ cm}^{-3}$ . The distribution of carriers is strongly shifted to the  $\Sigma$  band.

## V. THEORETICAL CALCULATIONS

The theoretical description of the magnetic properties of the Pb-Sn-Mn-Te semimagnetic semiconductor is based on the following model. Paramagnetic  $\text{Mn}^{2+}$  ions with spin moment  $S = \frac{5}{2}$  are statistically distributed in the fcc magnetic sublattice of the crystal lattice of Pb-Sn-Mn-Te. The magnetic moments are coupled by the long-range indirect (RKKY) exchange interaction via the

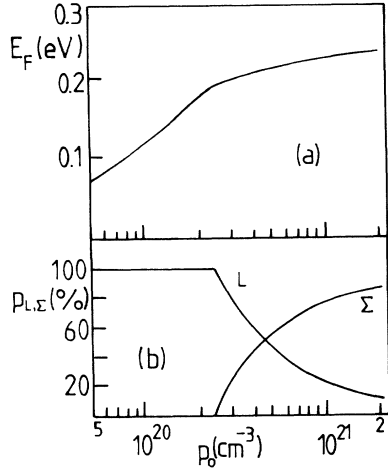


FIG. 11. The dependence of the Fermi energy of  $\text{Pb}_{0.25}\text{Sn}_{0.72}\text{Mn}_{0.03}\text{Te}$  on the total carrier concentration  $p_0$ . (b) presents the carrier-concentration dependent distribution of holes between bands of light and heavy holes.

free holes. In the case of nearest-neighbor spins, a weak antiferromagnetic superexchange interaction, usually present in IV-VI SMSC, should also be taken into account.

The calculations of the paramagnetic Curie temperature ( $\theta$ ) are based on the Heisenberg isotropic Hamiltonian:

$$H = - \sum_{(i,j)} I(R_{ij}) \mathbf{S}_i \cdot \mathbf{S}_j, \quad (4)$$

where  $I(R_{ij})$  is the exchange integral between two magnetic moments  $\mathbf{S}_i$  and  $\mathbf{S}_j$  separated by the distance  $R_{ij}$ . The summation should be carried out through the whole set of possible pairs of spins. Our calculations show that, in the case of the RKKY interaction in Pb-Sn-Mn-Te, one has to take into account the coupling between Mn ions separated by the distances  $R_{ij} \leq 6a_0$ , where  $a_0$  is the lattice constant of Pb-Sn-Mn-Te.

In the RKKY mechanism, the exchange integral is given by Eq. (5):<sup>24</sup>

$$I(R_{ij}) = \frac{J_{sd}^2 (k_F a_0)^6}{64 E_F \pi^3} F_{\text{RK}}(2k_F R_{ij}) \exp\left[-\frac{R_{ij}}{\lambda}\right], \quad (5)$$

where  $J_{sd}$  is the exchange integral between localized manganese spin and free carriers,  $E_F = \hbar^2 k_F^2 / 2m_0$  is the Fermi energy,  $a_0$  is the lattice constant,  $\lambda$  is the carrier mean free path, and

$$F_{\text{RK}}(x) = \frac{\sin(x) - x \cos(x)}{x^4}$$

is the Ruderman-Kittel (RK) function.

In the magnetic fcc sublattice, only discrete distances between spins are possible and are given by the formula  $R_i = a_0 \sqrt{i}/2$ , where  $i = 1, 2, 3, \dots$ . Equation (5) now can be written in the following form:

$$I(R_i) = \frac{m_d^* J_{sd}^2 a_0^2}{128 \hbar^2 \pi^3 i^{3/2}} [\sin(c\sqrt{i}) - c\sqrt{i} \cos(c\sqrt{i})] \times \exp\left[-\frac{a_0 \sqrt{i}}{\lambda \sqrt{2}}\right]. \quad (6)$$

Here  $c = \sqrt{2} k_F a_0$ , and  $m_d^*$  is the density-of-states effective mass of carriers on the Fermi surface (in one energy valley). One can see that the RKKY exchange integral depends on the exchange constant between the free carriers and the localized moment on the effective mass of density of states and on the number of carriers (via the Fermi vector  $k_F$ ).

Equation (6), describing the strength of the RKKY interaction, contains the phenomenological damping factor depending on the mobility of carriers.<sup>24</sup> Due to the fact that conducting carriers in Pb-Sn-Mn-Te have rather low mobilities, this factor may be important. In the case of the Pb-Sn-Mn-Te semimagnetic semiconductors, the RKKY interaction is mediated by two kinds of carriers: light holes from the  $L_6^-$  band and heavy holes from the  $\Sigma$  band. The total RKKY exchange integral ( $I_{\text{RKKY}}$ ) depends on the concentration of light ( $p_L$ ) and heavy holes ( $p_\Sigma$ ):

$$I_{\text{RKKY}}(p, R_i) = 4I_L(p_L, R_i) + 12I_\Sigma(p_\Sigma, R_i). \quad (7)$$

Here  $I_L(p_L, R_i)$  and  $I_\Sigma(p_\Sigma, R_i)$  are the RKKY exchange integrals due to light ( $L$ ) and heavy ( $\Sigma$ ) holes, respectively. These integrals are described by Eqs. (5) and (6) taking into account different effective masses of both kinds of carriers. Factors 4 and 12 appear in Eq. (7) due to the many-valley energy band structure of Pb-Sn-Mn-Te. Each energy valley is an independent channel for the RKKY mechanism. To calculate the Fermi wave vector of carriers, one should take the number of carriers per one valley (i.e.,  $p_L/4$  for light holes and  $p_\Sigma/12$  for heavy holes).

The experimentally measured parameter, the paramagnetic Curie temperature ( $\theta$ ), is, in the case of the random magnetic system, given by

$$k_B \theta = \frac{2}{3} S(S+1) y \sum_{(i)} z_i I_t(R_i), \quad (8)$$

where  $y$  is the concentration of magnetic ions,  $z_i$  is the number of atoms in the fcc lattice which are separated from the given atom by the distance  $R_i$ , and  $I_t(R_i)$  is the total exchange integral.

In the framework of our model, the total exchange integral, which couples two spins separated by the distance  $R_i$ , consists of two RKKY mechanism contributions (due to carriers from the  $L$  and from the  $\Sigma$  bands) and in the case of nearest-neighbor spins, the antiferromagnetic (AF) contribution due to the superexchange mechanism. The latter effect is described by the exchange integral  $I_{\text{AF}}$  which will be estimated in Sec. VI based on our experimental data. The total exchange integral is now given by the following expression:

$$I_t(R_i) = \begin{cases} I_{\text{RKKY}}(p, R_i) - I_{\text{AF}} & \text{for } i = 1, \\ I_{\text{RKKY}}(p, R_i) & \text{for } i \geq 2. \end{cases} \quad (9)$$



We have now the following formulas for the paramagnetic Curie temperature of Pb-Sn-Mn-Te:

$$\theta = \theta_{AF} + \theta_{RKKY}, \quad (10)$$

$$\theta_{AF} = -\frac{2}{3}S(S+1)y z_1 I_{AF}, \quad (11)$$

$$\theta_{RKKY} = \frac{2}{3}S(S+1)y \sum_{i=1} z_i I_{RKKY}(p, R_i). \quad (12)$$

In our model the superexchange contribution to the paramagnetic Curie temperature is carrier-concentration independent. The typical carrier-concentration dependence of the RKKY contribution is presented in Fig. 8. This curve was calculated for the case of the band parameters of the  $L_6^-$  band of  $\text{Pb}_{0.25}\text{Sn}_{0.72}\text{Mn}_{0.03}\text{Te}$ . One can notice the following two characteristic properties of this dependence. There is a maximum at carrier concentration (per one valley)  $p \simeq 7 \times 10^{20} \text{ cm}^{-3}$ . At low carrier concentrations, the paramagnetic Curie temperature depends on a carrier concentration as  $\theta \sim p^{1/3}$ .

The calculations of the carrier-concentration dependence of the paramagnetic Curie temperature were done in the following way. For each total carrier concentration ( $p_0$ ) we calculate the Fermi energy and the distribution of carriers between the bands of light and heavy holes according to the condition:

$$p_0 = p_L(E_F) + p_\Sigma(E_F).$$

Based on the model of the band structure presented in Sec. IV, we also determine the effective mass of light holes.<sup>22</sup> To calculate the RKKY exponential damping factor, we also need the values of microscopic mobilities of both kinds of carriers. These parameters can be determined based on the experimentally measured Hall mobilities which, in the case of  $\text{Pb}_{0.25}\text{Sn}_{0.72}\text{Mn}_{0.03}\text{Te}$ , follow a phenomenological law  $\mu = 300/p$ , where  $\mu$  is the Hall mobility in units  $\text{cm}^2/\text{Vs}$  and  $p$  is the Hall carrier concentration in units  $10^{20} \text{ cm}^{-3}$ . The microscopic mobilities can be determined using the calculated distribution of carriers and the mobility ratio  $b = \mu_\Sigma/\mu_L$ . The latter parameter was determined based on the analysis of the temperature and carrier-concentration dependence of the two-carrier Hall constant and is equal to  $b = 0.2$ .<sup>21,25</sup>

Theoretical calculations are based on the total carrier concentration ( $p_0$ ), whereas the experimental data are usually presented as a function of the low-temperature Hall concentration ( $p$ ). To compare theory and experimental data one has to recalculate the total carrier concentrations to the Hall one using the two-carrier effective Hall factor defined as  $r^* = p_0/p$ . The value of this parameter depends on the carrier concentration and we calculate it for each carrier concentration during the theoretical calculations of the carrier-concentration dependence of the Curie temperature. We use a simple model<sup>22,25</sup> according to which the Hall factor of the light holes is determined by the anisotropy of the  $L_6^-$  band and the carrier concentration dependence of the effective Hall factor is mostly due to redistribution of carriers between valence bands. The results of our model calculations show that the difference between total and Hall carrier concentration is typically less than 30%.

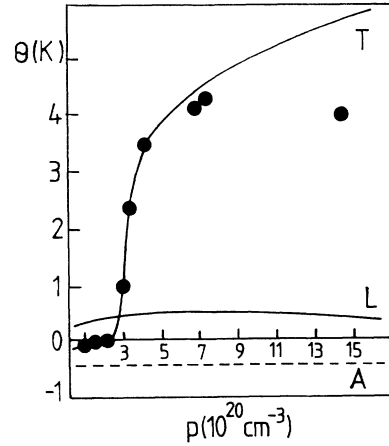


FIG. 12. The results of the theoretical calculations of the carrier-concentration dependence of the paramagnetic Curie temperature of  $\text{Pb}_{0.25}\text{Sn}_{0.72}\text{Mn}_{0.03}\text{Te}$ . The dashed line (A) presents the contribution due to superexchange interaction between nearest-neighbor spins. The solid line (L) describes the contribution due to the RKKY interaction via light holes (L). The total effect (i.e., the RKKY contributions due to the light and heavy holes and the contribution due to the superexchange interaction) is presented by the solid line (T).

## VI. DISCUSSION AND CONCLUSIONS

The results of the theoretical calculations of the carrier-concentration dependence of the paramagnetic Curie temperature of  $\text{Pb}_{0.25}\text{Sn}_{0.72}\text{Mn}_{0.03}\text{Te}$  are presented in Fig. 12. One can see that the dominant physical mechanism determining the magnetic properties of this material is the RKKY exchange interaction via heavy holes. The RKKY contribution due to the light holes from the  $L_6^-$  band is an order of magnitude smaller due to relatively small effective mass of density of states. To obtain a correct theoretical description of the experimental data for samples with carrier concentrations  $p < 3 \times 10^{20} \text{ cm}^{-3}$ , we have to assume that the antiferromagnetic interaction between nearest-neighbor spins is described by the exchange integral  $I_{AF} = 0.25 \pm 0.05 \text{ K}$ . This value agrees reasonably well with experimental data for another IV-VI SMSC.<sup>6</sup> The role of this weak antiferromagnetic interaction is to compensate the small positive contribution to the paramagnetic Curie temperature connected with the RKKY interaction via light holes. The latter mechanism predicts the paramagnetic Curie temperature  $\theta \simeq +0.5 \text{ K}$  that is not observed experimentally. The paramagnetic Curie temperatures of the samples of Pb-Sn-Mn-Te with a carrier concentration  $p < 3 \times 10^{20} \text{ cm}^{-3}$  are close to zero.

Comparing the results of the theoretical calculations with the experimental data (Fig. 12), one can conclude that the model of magnetic properties of Pb-Sn-Mn-Te presented in Sec. V describes well the experimental data in the wide carrier-concentration range  $p = 8 \times 10^{19}$  to  $7 \times 10^{20} \text{ cm}^{-3}$ . In the case of samples with very large carrier concentrations, the decrease of the Curie tempera-

ture with an increasing carrier concentration is not correctly reproducible in our calculations. The maximum, which usually appears on the carrier-concentration characteristics of the Curie temperature determined by the RKKY interaction, is observed at a carrier concentration per one energy valley  $p \approx 7 \times 10^{20} \text{ cm}^{-3}$ . It means that the total carrier concentration of heavy holes should be equal to  $p_{\Sigma} \approx 8 \times 10^{21} \text{ cm}^{-3}$ . It is much higher than the highest concentrations obtained in the samples of Pb-Sn-Mn-Te.

In our opinion, the experimentally observed decrease of the Curie temperature may be qualitatively understood based on the damping effect of the exponential factor in the RKKY mechanism. Due to the fact that, with an increasing carrier concentration, we observe experimentally a rather strong decrease of the mobility of carriers ( $\mu \sim 1/p$ ), one can also expect a significant reduction of the carrier mean free path and a decrease of the Curie temperature. The damping factor in the RKKY interaction influences the magnitude of the interaction when the mean free path is comparable with the mean interdistance between magnetic ions. In the case of Pb-Sn-Mn-Te, this condition means that the effect may be observed if the mobilities of the carriers are in the range of  $\mu \leq 10 \text{ cm}^2/\text{V s}$ . Such low mobilities are observed in the case of heavy holes in Pb-Sn-Mn-Te. However, the calculated mean free path of heavy holes decreases too slowly with the increasing carrier concentration to account for the observed experimental behavior.

The theoretical curve fitting the experimental data was calculated with the exchange constant equal to  $J_{sd} = 100 \pm 5 \text{ meV}$ . This value is comparable with exchange constants observed in other  $p$ -type IV-VI SMSC (Pb-Mn-Te and Pb-Mn-Se).<sup>26,27</sup>

Finally, we would like to discuss the assumptions on which our theoretical calculations presented above are based. We do not take into account the possible effect of the nonparabolicity and anisotropy of the band of light holes on the RKKY mechanism. This effect may influence only the small contribution of light holes to the total RKKY exchange integral and is not crucial in the theoretical calculations of the Curie temperature of Pb-Sn-Mn-Te. The energy dispersion relation in the band of heavy holes is parabolic and this dominant contribution is calculated correctly. Due to the lack of the experimental data, we assume also that the exchange constants of both light and heavy holes are the same.

Our experimental data strongly suggest that the low-temperature magnetic phase observed in Pb-Sn-Mn-Te ( $y=0.03$ ) is ferromagnetic. This conclusion was recently confirmed by neutron-diffraction measurements on the related material  $\text{Sn}_{1-x}\text{Mn}_x\text{Te}$  ( $y=0.03$  and  $0.06$ ).<sup>28</sup> Generally, in diluted magnetic systems with a RKKY interaction, the formation of the spin-glass phase is very probable.<sup>29</sup> Our calculations show that, in

$\text{Pb}_{0.25}\text{Sn}_{0.72}\text{Mn}_{0.03}\text{Te}$  ( $p = 7 \times 10^{20} \text{ cm}^{-3}$ ), the RKKY interaction between magnetic moments separated by the distance  $R < 20 \text{ Å}$  is ferromagnetic. The mean distance between magnetic ions in this material is about  $13 \text{ Å}$ . This situation favors the formation of the ferromagnetic phase. However, in more magnetically diluted crystals, in which the mean distance between magnetic ions is larger, the effect of the oscillating sign of the RKKY interaction may be important and lead to the formation of spin-glass phase. The first experimental evidences that this mechanism is really effective in Pb-Sn-Mn-Te were recently obtained in  $\text{Pb}_{0.26}\text{Sn}_{0.72}\text{Mn}_{0.02}\text{Te}$  and  $\text{Sn}_{0.98}\text{Mn}_{0.02}\text{Te}$  with a carrier concentration  $p \geq 10^{21} \text{ cm}^{-3}$ .<sup>30</sup> One can also expect interesting magnetic properties of the samples with a threshold carrier concentration  $p = p_c$ . The reduced magnitude of the RKKY interaction should increase the role of weak short-range antiferromagnetic interactions. The possible effects resulting from the competition between these two exchange mechanisms should be important at temperatures  $T \leq 1 \text{ K}$  and, as yet, were not studied experimentally.

Summarizing our experimental and theoretical studies we would like to stress the following points.

(1) In the Pb-Sn-Mn-Te semimagnetic semiconductor, we observed a transition from a paramagnetic to ferromagnetic phase induced by a carrier concentration.

(2) The abrupt transition to a ferromagnetic phase is governed by a RKKY mechanism involving two types of carriers (light and heavy holes) with a dominating role of heavy holes.

(3) Detailed knowledge of the energy band structure deduced from the semiconductor properties of Pb-Sn-Mn-Te is a firm confirmation of our interpretation. It also illustrates the importance of the band structure (not only a carrier concentration) in the RKKY interaction.

(4) The general physical description of the magnetic properties of  $\text{Pb}_{0.25}\text{Sn}_{0.72}\text{Mn}_{0.03}\text{Te}$  should also be valid for materials with different host compositions and different concentrations of manganese ions, as far as these materials have a band structure similar to the one presented in Fig. 10. Recent experimental data obtained for Sn-Mn-Te (Ref. 31) and for  $\text{Pb}_{1-x}\text{Sn}_x\text{Mn}_y\text{Te}$  with composition  $x=0.72$ ,  $y=0.06$ , and  $y=0.08$  (Ref. 32), show that, indeed, the carrier-concentration induced ferromagnetism is observed in the wide range of chemical compositions of Pb-Sn-Mn-Te semimagnetic semiconductors.

#### ACKNOWLEDGMENTS

We would like to thank A. Szczerbakow for the preparation of our crystals, A. Lenard, A. Lewicki, and Z. Tarnawski for specific-heat measurements, and M. Leszczyński for the x-ray analysis of our samples. Helpful discussions with W.J.M. de Jonge and H.J.M. Swagten are also acknowledged.

<sup>1</sup>G. Nimtz, and B. Schlicht, *Narrow Gap Semiconductors*, Vol. 98 of *Springer Tracts in Modern Physics* (Springer, Berlin, 1983).

<sup>2</sup>R. R. Gałązka, in *Proceedings of the 14th International Confer-*

*ence on the Physics of Semiconductors, Edinburgh, 1978*, IOP Conf. Ser. 43, edited by B. L. H. Wilson (IOP, London, 1978), p. 133.

<sup>3</sup>G. Bauer, in *Diluted Magnetic Semiconductors*, edited by R. L.

- Aggarwal, J. K. Furdyna, and S. von Molnar (Materials Research Society, Pittsburgh, 1987), Vol. 89, p. 107.
- <sup>4</sup>M. Kossut, *Semiconductors and Semimetals*, edited by J. K. Furdyna, J. Kossut (Academic, Boston, 1988), Vol. 25.
- <sup>5</sup>G. Karczewski, M. von Ortenberg, Z. Wilamowski, W. Dobrowolski, and J. Niewodniczańska-Zawadzka, *Solid State Commun.* **55**, 249 (1985).
- <sup>6</sup>M. Górska, and J. R. Anderson, *Phys. Rev. B* **38**, 9120 (1988).
- <sup>7</sup>M. Escorne, A. Mauger, J. T. Tholence, and R. Triboulet, *Phys. Rev. B* **29**, 6306 (1984).
- <sup>8</sup>J. Cohen, A. Globa, P. Mollard, H. Rodot, and M. Rodot, *J. Phys. (Paris) Colloq.* **29**, C4-143 (1968).
- <sup>9</sup>M. Inoue, Hoong Kun Fun, M. Fulcuoka, and H. Yagi, in *Proceedings of the 15th International Conference on Physics, Semiconductors, Kyoto, 1980*, edited by S. Tanaka (Physical Society of Japan, Tokyo, 1989), p. 835.
- <sup>10</sup>M. Escorne and A. Mauger, *Solid State Commun.* **31**, 893 (1979).
- <sup>11</sup>T. Hamasaki, *Solid State Commun.* **32**, 1069 (1979).
- <sup>12</sup>M. P. Mathur, D. W. Deis, C. K. Jones, A. Paterson, and W. J. Carr, Jr., *J. Appl. Phys.* **42**, 1693 (1971).
- <sup>13</sup>R. W. Cochrane, F. T. Hedgcock, and J. O. Ström-Olsen, *Phys. Rev. B* **9**, 3013 (1974).
- <sup>14</sup>T. Story, R. R. Gałazka, R. B. Frankel, and P. A. Wolff, *Phys. Rev. Lett.* **56**, 777 (1986).
- <sup>15</sup>T. Story, L. Świerkowski, G. Karczewski, W. Staghun, and R. R. Gałazka, in *Proceedings of the 19th International Conference on Physics Semiconductors, Warsaw, 1988*, edited by W. Zawadzki (Institute of Physics, Warsaw, 1989), p. 1567.
- <sup>16</sup>T. Story, A. Lewicki, and A. Szczerbakow, *Acta Phys. Pol. A* **67**, 317 (1985).
- <sup>17</sup>T. Story, A. Lenard, and R. R. Gałazka, *Acta. Phys. Pol. A* **69**, 1005 (1986).
- <sup>18</sup>R. R. Gałazka, S. Nagata, and P. H. Keesom, *Phys. Rev. B* **22**, 3344 (1980).
- <sup>19</sup>T. Suski, J. Igalson, and T. Story, *J. Magn. Magn. Mater.* **66**, 325 (1987).
- <sup>20</sup>H. J. M. Swagten, W. J. M. de Jonge, R. R. Gałazka, P. Warmenbol, and J. T. Devreese, *Phys. Rev. B* **37**, 9907 (1988).
- <sup>21</sup>T. Story, G. Karczewski, and L. Świerkowski, *Acta Phys. Pol. A* **75**, 277 (1989).
- <sup>22</sup>G. Karczewski, L. Świerkowski, T. Story, A. Szczerbakow, J. Niewodniczańska-Blinowska, and G. Bauer, *Semicond. Sci. Technol.* (to be published).
- <sup>23</sup>C. R. Hewes, M. S. Adler, and S. D. Senturia, *Phys. Rev. B* **7**, 5197 (1973).
- <sup>24</sup>D. C. Mattis, *The Theory of Magnetism* (Springer, Berlin, 1981), Part 1.
- <sup>25</sup>T. Story, Philos. Dr. thesis, Institute of Physics, Warsaw, 1988 (unpublished).
- <sup>26</sup>G. Toth, J. Y. Loloup, and H. Rodot, *Phys. Rev. B* **1**, 4573 (1973).
- <sup>27</sup>L. Kowalczyk, *Acta Phys. Pol. A* **77**, 191 (1990).
- <sup>28</sup>C. W. H. M. Vennix, E. Frikkee, H. J. M. Swagten, K. Kopinga, and W. J. M. de Jong, in *Proceedings of the 35th Annual Conference on Magnetism and Magnetic Materials, San Diego, 1990* [*J. Appl. Phys.* (to be published)].
- <sup>29</sup>J. A. Mydosh and G. J. Niewenhuys, in *Ferromagnetic Materials*, edited by E. P. Wohlfarth (North-Holland, Amsterdam, 1980), p. 71.
- <sup>30</sup>H. J. M. Swagten, T. Story, R. J. T. van Kempen, M. M. H. Willekens, and W. J. M. de Jonge, in *Proceedings of the 35th Annual Conference on Magnetism and Magnetic Materials, San Diego, 1990* [*J. Appl. Phys.* (to be published)].
- <sup>31</sup>W. J. M. de Jong, H. J. M. Swagten, S. J. E. A. Eltink, and N. M. J. Stoffels, *Proceedings of the International Conference on Narrow Gap Semiconductors and Related Materials, Gaithersburg, 1989* [*Semicond. Sci. Technol.* **5**, S131 (1990)].
- <sup>32</sup>T. Story, G. Karczewski, L. Świerkowski, M. Górska, and R. R. Gałazka, *Proceedings of the International Conference on Narrow Gap Semiconductors and Related Materials, Gaithersburg, 1989* [*Semicond. Sci. Technol.* **5**, S138 (1990)].